Cancer Cell
Article

Neuregulin-1-Mediated Autocrine Signaling Underlies Sensitivity to HER2 Kinase Inhibitors in a Subset of Human Cancers

Timothy R. Wilson,[1,2] Diana Y. Lee,[1] Leanne Berry,[2] David S. Shames,[2] and Jeff Settleman[1,2,*]
[1]Massachusetts General Hospital Cancer Center and Harvard Medical School. Building 149, 13th Street, Charlestown, Boston, MA 02129, USA
[2]Genentech Inc., 1 DNA Way, South San Francisco, CA 94080, USA
*Correspondence: settleman.jeffrey@gene.com
DOI 10.1016/j.ccr.2011.07.011

SUMMARY

HER2 kinase inhibitors, such as lapatinib, have demonstrated clinical efficacy in *HER2*-amplified breast cancers. By profiling nearly 700 human cancer cell lines, we identified a subset of non-*HER2* amplified cancer cells with striking sensitivity to HER2 kinase inhibition—particularly from head and neck tumors. These cells were found to depend on a neuregulin-1 (NRG1)-mediated autocrine loop driving HER3 activation, which can be disrupted by lapatinib. Elevated NRG1 expression and activated HER3 are strongly associated with lapatinib sensitivity in vitro, and these biomarkers were enriched in a subset of primary head and neck cancer samples. The findings suggest that patients with NRG1-driven tumors lacking *HER2* amplification may derive significant clinical benefit from HER2:HER3-directed therapies.

INTRODUCTION

The dependency of tumor cells on a single activated protein or pathway activity, despite the likely accumulation of numerous oncogenic mutations, is referred to as "oncogene addiction" (Weinstein et al., 1997), and this phenomenon has been demonstrated in a variety of murine cancer models that rely on the sustained expression of the transforming oncogene for tumor maintenance (Sharma and Settleman, 2007). This reliance on a single activated oncoprotein implicates a potential "Achilles' heel" in such cells, which has been successfully exploited by the discovery and development of anticancer agents that selectively target these critical proteins and associated signaling pathways to yield clinical benefit in molecularly defined patient populations. For example, in breast cancer, approximately 25% of patients demonstrate genomic amplification of *HER2*, encoding the human epidermal growth factor (EGF) receptor (EGFR)-related kinase, which can be targeted by the HER2 receptor antibody trastuzumab (Slamon et al., 2001), frequently leading to clinical benefit. Similarly, nonsmall cell lung cancers (NSCLCs) that harbor activating EGFR kinase domain mutations are likely to respond to the selective EGFR kinase inhibitors erlotinib and gefitinib (Sequist and Lynch, 2008).

The HER family of proteins—HER1 (EGFR), HER2, HER3, and HER4—belongs to the superfamily of receptor tyrosine kinases (RTKs) (Holbro and Hynes, 2004). Activation of HER receptors is largely controlled by ligand binding, which induces formation of homo- and heterodimers, and subsequent activation of kinase activity. This leads to phosphorylation of specific sites in the cytoplasmic tail and recruitment of protein adaptors that engage downstream survival and proliferation pathways (Bose and Zhang, 2009). Although they share several structural and functional features, there are notable differences among the HER family members. First, HER2 has no known ligand and has been proposed to be the "preferred" binding partner for the other family members due to its open structure (Garrett et al., 2003). Second, HER3, although catalytically inactive, or weakly active (Shi et al., 2010), cannot form homodimers but contains

Significance

Several mutationally activated kinases are clinically validated cancer drug targets. Consequently, there is rapidly growing interest in tumor genotyping to prospectively identify patients most likely to benefit from these agents. However, genomic testing may not capture all patients who might derive benefit from such medicines because oncogenic kinase-mediated pathways do not necessarily require mutational activation. We identified a significant fraction of tested cancer cell lines driven by an autocrine-signaling loop in which the HER3 ligand neuregulin-1 promotes malignancy by engaging the HER2 kinase. In these cases HER2 inhibition effectively blocks tumor cell growth. We describe a biomarker associated with drug response, suggesting a diagnostic strategy to identify patients with non-*HER2* amplified tumors that may benefit from established HER2:HER3-targeted therapies.

six p85 binding sites in the cytoplasmic domain that can engage the PI3K survival pathway (Berger et al., 2004; Zhang et al., 1996). Among the various dimers that can be formed within the HER family, the HER2:HER3 heterodimer has been suggested to transduce the strongest signaling response (Tzahar et al., 1996). Recently, a critical role for HER3 has been demonstrated in *HER2*-amplified breast cancer-derived cell lines (Lee-Hoeflich et al., 2008).

Overexpression or mutational activation of HER proteins may not be the only mechanisms by which HER signaling pathways can be engaged in tumor cells and, consequently, impact the response to pathway-targeted therapeutics. Thus, cancer cells can produce various EGF-related ligands that result in autocrine activation of survival and proliferation signals (Salomon et al., 1995). For example, a recent study demonstrated that autocrine production of the EGFR ligand amphiregulin is associated with sensitivity of EGFR wild-type cancer cells to EGFR-targeted therapies (Yonesaka et al., 2008). Similarly, a RNAi screen identified HER3 as a therapeutic target in ovarian cancer via its activation by a neuregulin-1 (NRG1) autocrine loop (Sheng et al., 2010). In light of these various HER activation mechanisms, several therapeutic strategies have been developed to inhibit HER-mediated signaling (Hynes and Lane, 2005). These include antibodies that bind the extracellular domain (ECD) of HER proteins, such as cetuximab, which binds EGFR, and trastuzumab, which binds HER2, as well as small molecule tyrosine kinase inhibitors (TKIs), such as erlotinib, which inhibits EGFR, and lapatinib, which inhibits EGFR and HER2. Following successful clinical testing these molecules have been FDA approved for the treatment of cancer patients. Thus, erlotinib is used to treat metastatic NSCLC patients that have progressed on chemotherapy (Smith, 2005), and lapatinib is used to treat HER2-positive metastatic breast cancer patients that have progressed on trastuzumab therapy (Medina and Goodin, 2008).

The ability to prospectively identify patients likely to respond to the various molecularly targeted therapies is critical to their optimal clinical utility. Fortunately, human tumor-derived cell lines have proven to be a useful platform in which to identify such predictive biomarkers associated with oncogene addiction (Sharma et al., 2010). We have previously described a high-throughput platform for profiling the sensitivity of human tumor cell lines to a variety of kinase inhibitors, demonstrating the ability of this platform to reveal clinically relevant biomarker-response relationships (McDermott et al., 2007). For example, we recently described the ability of this approach to establish ALK (anaplastic lymphoma kinase)-associated chromosomal translocations as a sensitizing genotype in the context of treatment with a selective ALK inhibitor (McDermott et al., 2008), prompting successful clinical testing of an ALK inhibitor in genomically defined lung cancer patients (Kwak et al., 2010).

To date, we have employed this platform to test approximately 700 solid tumor-derived cell lines with a variety of compounds that correspond to clinically approved cancer drugs, investigational compounds, or promising preclinical agents. Because many of these candidate therapeutic compounds hold promise as effective anticancer drugs, preclinical studies are warranted to identify molecularly defined subclasses of tumors that can be used to guide their clinical development Here, we describe the use of this platform to identify a biomarker-defined subset of tumor cells that demonstrate sensitivity to HER2-targeted kinase inhibitors that is independent of genomic *HER2* status.

RESULTS

A Subset of Non-*HER2* Amplified Cancer Cell Lines Is Sensitive to HER2 Kinase Inhibition

We profiled the sensitivity of 690 cancer cell lines, derived from multiple tissue types (see Figure S1 available online), to the investigational irreversible dual EGFR and HER2 TKI HKI-272 (Figure 1A and Table S1). Whereas the vast majority of HKI-272-treated cell lines were largely treatment refractory, a small proportion of cell lines exhibited either moderate sensitivity (12.2%) or extreme sensitivity (1.3%) to HKI-272. The most sensitive cell lines are represented in Figure 1A. To determine the contribution of EGFR dependency to HKI-272 sensitivity, we performed a parallel analysis of the same cell line panel with the EGFR-selective TKI erlotinib. As expected, among the HKI-272-sensitive cell lines, we identified several lines with *HER2* gene amplification, such as the UACC-893 and SKBR3 breast cancer cell lines and the NCI-N87 gastric cancer cell line. We also identified cell lines that harbor activating *EGFR* mutations, such as the NSCLC cell lines: H3255, PC-9, HCC-827, and PC-14. These *EGFR*-mutated cells also displayed sensitivity to erlotinib, indicating that the observed sensitivity of those cells to HKI-272 was due to EGFR kinase inhibition and not to HER2 kinase inhibition.

In addition to the treatment-sensitive lines that could be explained by the presence of EGFR or HER2 activation, we identified an additional subset of HKI-272-sensitive cell lines that was refractory to erlotinib and does not harbor *HER2* or *EGFR* amplifications or mutations. The single-most HKI-272-sensitive cell line was the erlotinib-refractory MDA-MB-175-VII breast cancer cell line, and does not exhibit *HER2* amplification. Significantly, this cell line reportedly expresses a NRG1 fusion protein, as a consequence of a chromosomal translocation, that results in the aberrant autocrine activation of HER3 (Schaefer et al., 1997). Other HKI-272-sensitive, erlotinib-refractory cell lines include those derived from skin, kidney, bone, uterus, and intestine. Notably, this subset was enriched for cell lines derived from head and neck tumors (Table S2).

As a complementary approach, we carried out a secondary screen using the FDA-approved drug lapatinib, a dual EGFR/HER2 inhibitor, on a panel of 22 cell lines arbitrarily selected from among 34 of the identified HKI-272-sensitive cell lines that were also largely erlotinib refractory (as indicated in Figure 1A). These cells could be categorized into three groups: sensitive (response below 1 μM), moderately sensitive (response between 1 and 5 μM), and refractory (no response) (Figure 1B). IC_{50} values are listed in Figure 1A. Because lapatinib is reportedly one of the most selective TKIs developed to date (Bantscheff et al., 2007), the lack of complete correlation with the HKI-272 sensitivity profile observed in the large cell panel is likely to reflect off-target effects of this irreversible kinase inhibitor. Collectively, these results indicate that a subset of cancer cell lines displays sensitivity to HER2 kinase inhibition in the absence of *HER2* gene amplification.

A

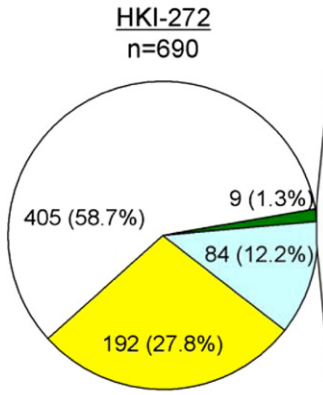

Cell Line	Tissue	HKI-272	Erlotinib	Her2 amp	EGFR mut	Unexplained sensitivity	Lapatinib IC50 (μM)
MDA-MB-175	Breast	0.055	0.713			X	0.48
H3255	NSCLC	0.092	0.085				
CAL-39	Cervix	0.118	0.322				
PC-9	NSCLC	0.170	0.074				
UACC-893	Breast	0.171	1.150				
KHM-3S	Lung	0.183	0.195				
NCI-N87	Stomach	0.194	0.812				
CHL-1	Skin	0.195	0.873			X	0.10
JHH-1	Liver	0.200	0.394				
LU65B	NSCLC	0.203	0.462				
OE19	Esoph	0.213	0.980				
HuCCT1	Liver	0.242	0.818			X	8.9
NUGC-2	Stomach	0.252	0.281				
CS1R	Bone	0.255	1.081			X	4.9
PCI-6A	H&N	0.257	0.524			X	0.07
H3118	H&N	0.259	0.301				
PCI-4A	H&N	0.259	0.386				
MFE-319	Uterus	0.266	0.598			X	ND
JHU-029	H&N	0.267	0.463			X	ND
SCC-9	H&N	0.269	0.402				
DoTc2 4510	Cervix	0.269	0.479			X	1.6
DLD-1	Intestine	0.269	0.713			X	>10
PCI-4B	H&N	0.276	0.769			X	ND
HCC1419	Breast	0.278	0.860				
HCC-827	NSCLC	0.282	0.282				
EFM-192A	Breast	0.284	0.899				
PC-14	NSCLC	0.290	0.236				
HN	H&N	0.293	0.550			X	3.3
PE/CA-PJ15	H&N	0.294	0.659			X	ND
SN-12C	Kidney	0.295	0.671			X	3.2
LU65A	NSCLC	0.296	0.518			X	ND
FaDu	H&N	0.298	0.604			X	1.2
BHY	H&N	0.301	0.454			X	2.5
OVMIU	Ovary	0.307	0.483			X	ND
Calu-3	NSCLC	0.309	0.634				
BICR 31	H&N	0.313	0.520				
CAL 27	H&N	0.317	0.699			X	3.9
DU 145	Prostate	0.323	0.702			X	>10
HSC-3	H&N	0.325	0.772			X	3.3
AU565	Breast	0.332	1.068				
A2.1	Panc	0.333	0.860			X	>10
KYSE-520	Esoph	0.335	0.409		amp		
H513	Lung	0.335	0.589			X	ND
HSC-2	H&N	0.345	0.582			X	>10
OVTOKO	Ovary	0.348	0.517			X	ND
NCI-H2347	NSCLC	0.352	0.800			X	>10
SNG-M	Uterus	0.358	0.900			X	3.4
PCI-15	H&N	0.361	0.740			X	ND
NCI-H661	NSCLC	0.371	1.005			X	>10
KYSE-450	Esoph	0.374	0.489				
JHU-028	H&N	0.375	0.924			X	ND
H292	Lung	0.384	0.411				
NCI-H1975	NSCLC	0.394	0.845				
BICR 22	H&N	0.402	0.866			X	ND
OSC-20	H&N	0.404	0.889			X	ND
LN-18	Brain	0.408	1.061			X	7.9
SK-BR-3	Breast	0.412	0.893				
NB69	Nerv Sys	0.412	1.022			X	4.4
SAT	H&N	0.414	0.801			X	0.16
Ca9-22	H&N	0.416	0.569		amp		

B

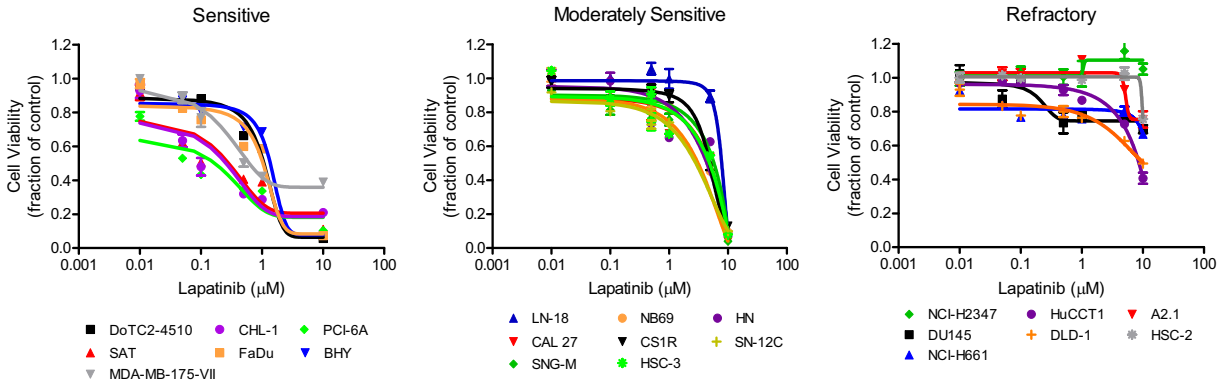

Figure 1. Large-Scale Cell Line Screening Identifies a Subset of Non-*HER2* Amplified Human Cancer Cell Lines Sensitive to HER2 Kinase Inhibitors

(A) Pie chart representing the cell sensitivity distribution of 690 human solid tumor-derived cell lines when tested for response to the dual EGFR and HER2 inhibitor HKI-272 (200 nM). The legend corresponds to the fraction of cells remaining (compared to control) following exposure to drug (72 hr). Details for the 8.5% of cell

Lapatinib Sensitivity Is Associated with Elevated pHER3

To establish the molecular mechanism underlying lapatinib sensitivity in the non-*HER2* amplified cell lines, we initially analyzed the expression of EGFR, HER2, and HER3, as well as the downstream effectors, AKT and ERK, in the 22 cell lines that were examined in the secondary screen. As a positive control, we included the *HER2*-amplified SKBR3 breast cancer cell line in the analysis. As anticipated, none of the cell lines analyzed, other than SKBR3, displayed *HER2* amplification (Figure 2A). In addition basal levels of pEGFR, pHER2, pAKT, and pERK were not correlated with response to lapatinib. Because previous reports have demonstrated a critical role for HER3 expression in *HER2*-amplified breast cancer cells (Lee-Hoeflich et al., 2008), we measured HER3 and pHER3 in the cell line panel. All seven of the highly lapatinib-sensitive cell lines exhibited elevated pHER3, four of eight of the moderately lapatinib-sensitive cell lines displayed elevated pHER3, and only one of seven lapatinib-refractory cell lines demonstrated detectable pHER3 (Figure 2A). Thus, elevated pHER3 was well correlated with response to lapatinib ($p = 0.0308$; Figure 2B). To determine whether lapatinib treatment could suppress pHER3 signaling in the lapatinib-sensitive and moderately sensitive groups, a subset of the cell lines was treated with either lapatinib or erlotinib for 2 hr. Lapatinib treatment, but not erlotinib treatment, strongly suppressed pHER3 as well as downstream AKT activation, suggesting that HER2 kinase, but not EGFR kinase, activity was driving downstream survival signals in the lapatinib-sensitive cells, via HER3 (Figure 2C; Figure S2A). In contrast, lapatinib failed to suppress pAKT in the two refractory cell lines analyzed.

Next, to determine whether the lapatinib-sensitive and moderately sensitive cell lines (referred to as lapatinib-sensitive cell lines from this point on) expressing elevated pHER3 are dependent on HER3 expression, we knocked down HER3 using two independent shRNAs. Lentiviral-mediated infection of CHL-1 cells with shRNAs targeting HER3 successfully depleted HER3 protein (Figure 2D). Significantly, decreasing HER3 in the lapatinib-sensitive cell lines demonstrating elevated pHER3 substantially inhibited cell proliferation (Figure 2D; Figure S2B). To control for potential RNAi-associated off-target effects, we also knocked down HER3 in the lapatinib-refractory cell line MCF-7, and no antiproliferative effect was observed. Because pEGFR and pHER2 were barely detectable in this subset of cell lines, we employed two complementary approaches to confirm a critical role for HER2:HER3 heterodimers in signaling to AKT in these cells. First, we treated CHL-1, FaDu, or SAT cells with trastuzumab (HER2-targeted), pertuzumab (HER2/3-targeted), or a HER3-directed antibody (Figure 2E; Figures S2C, and S2D). Pertuzumab and the HER3-directed antibody suppressed pHER3 and pAKT in these cells. Second, we used shRNAs to knock down each of the four HER family members. Because HER4 was undetectable in these cells, we assessed knockdown efficiency in MCF-7 cells (Figure S2E). Knockdown of HER3 suppressed pAKT in CHL-1 and FaDu cells (Figure 2F). Importantly, knockdown of HER2, but not EGFR or HER4, suppressed pHER3 and downstream pAKT signaling in these cells. Notably, the failure to readily detect pHER2 in these cell lines is consistent with the fact that HER3 has weak kinase activity and is unlikely to transphosphorylate HER2 in this setting. Consistent with a requirement for HER3 in the lapatinib-sensitive cell lines, they were also found to exhibit sensitivity to BEZ235, an inhibitor of PI-3 kinase, which couples HER3-mediated survival signals to AKT (Figures S2F and S2G). Together, these results suggest that HER2:HER3 heterodimers drive cell survival via PI-3 kinase in a subset of non-*HER2* amplified cancer cell lines and that this pathway can be effectively suppressed by agents that target HER2 kinase activity.

Lapatinib-Sensitive Cells Secrete a HER3-Activating Ligand

Activation of HER receptors occurs via ligand binding, resulting in homodimerization or heterodimerization with other HER proteins. To determine whether the lapatinib-sensitive cell lines secrete a HER ligand, we developed an assay using the EFM-19 breast cancer cell line as a "reporter" of HER3 activation. EFM-19 cells were selected because they demonstrate low basal levels of pHER3 but express HER3 and HER2 at levels similar to those seen in the lapatinib-sensitive MDA-MB-175-VII cell line (Figure 3A). Exposing EFM-19 cells to serum-free media conditioned by the MDA-MB-175-VII cell line, which expresses the NRG1 fusion protein, resulted in the expected phosphorylation of HER3, demonstrating the utility of this model to detect the secretion of HER3-activating ligands (Figure 3A).

We next determined whether media conditioned by the lapatinib-sensitive, pHER3-positive cell lines could activate HER3 in the EFM-19 model. Conditioned media from each of the tested lapatinib-sensitive cell lines activated HER3 in EFM-19 cells (Figure 3B). As before, pHER2 was undetectable in EFM-19 cells treated with conditioned media, further supporting the conclusion that HER3 does not transphosphorylate HER2 in this setting (data not shown). Next, we assessed the ability of conditioned media from the lapatinib-refractory cells from Figure 2A, and an extended panel of HKI-272-refractory cell lines (as determined from the original screen, with a lapatinib $IC_{50} > 5\ \mu M$; data not shown), to activate HER3 in EFM-19 cells. We found that only 6 of 16 refractory cell lines were able to activate HER3 in this assay. Furthermore, conditioned media from neither the *HER2*-amplified SKBR3 cell line nor the *EGFR*-mutated PC-9 cell line activated HER3 in EFM-19 cells. We next determined

lines with the highest degree of HKI-272 sensitivity are displayed in the chart to the right, which are ranked according to decreasing sensitivity. The corresponding sensitivity of these lines to the specific EGFR inhibitor erlotinib (200 nM) is also presented. Green boxes indicate known *HER2* amplification or EGFR mutation. *EGFR* amplification, where known, is indicated (amp). Red boxes indicate no mutations, and white boxes indicate unknown mutations. H&N, head and neck; Nerv Sys, nervous system; Esoph, esophagus; ND, not determined. "Unexplained sensitivity" refers to nonmutationally activated cell lines (EGFR or HER2) that were largely refractory to erlotinib and displayed a similar or greater HKI-272 response than that seen in *HER2*-amplified SKBR3 cells.

(B) Secondary screen using 22 out of a total of 34 arbitrarily selected HKI-272-sensitive, erlotinib-refractory cell lines showing the effect on cell viability of a second dual EGFR and HER2 inhibitor, lapatinib (72 hr). The cell lines were categorized into three groups: sensitive (response below 1 μM), moderately sensitive (response between 1 and 5 μM), and refractory (did not respond). The IC_{50} concentration (μM) for each cell line is shown in the final column in (A). Error bars represent mean ± SEM. See also Figure S1, and Tables S1 and S2.

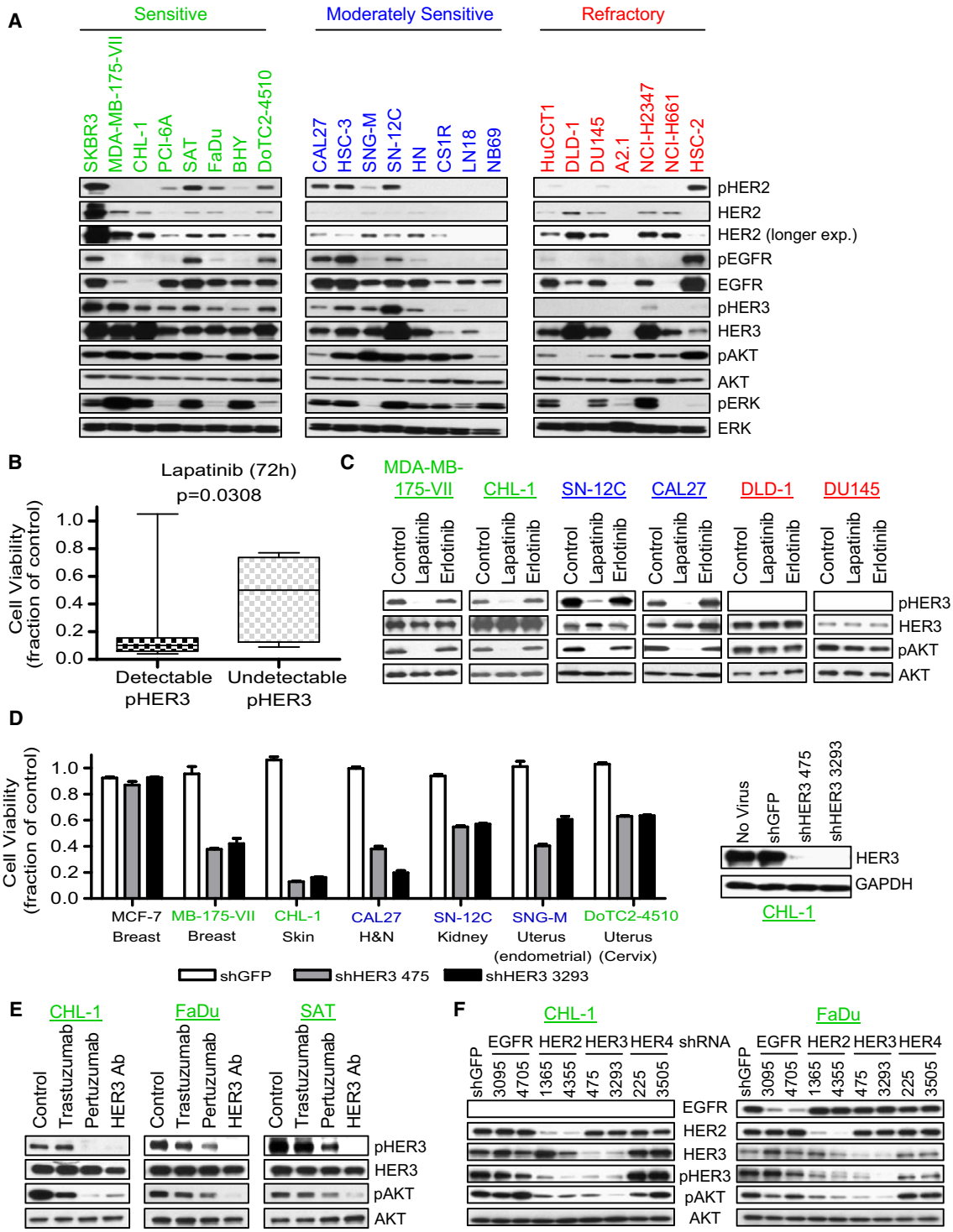

Figure 2. HER3 Mediates Lapatinib Sensitivity in Non-*HER2* Amplified Cancer Cell Lines

(A) Immunoblots indicating levels of pHER2, HER2, pHER3, HER3, pEGFR, EGFR, pAKT, AKT, pERK, and ERK in the lapatinib-sensitive, moderately sensitive, and refractory cell lines. As a control for HER2 overexpression, the *HER2*-amplified SKBR3 breast cancer cell line was included.

(B) Box and whisker plot comparing lapatinib sensitivity (cell proliferation, 72 hr) in the detectable pHER3 (n = 13) and nondetectable pHER3 (n = 9)-expressing cells. Statistical difference between the two groups was assessed using Student's t test (two-tailed, p = 0.0308). Cell lines belonging to the detectable pHER3 group include: CHL-1, MDA-MB-175-VII, PCI-6A, SAT, FaDu, BHY, DoTC2-4510, CAL27, HSC-3, SNG-M, SN12C, HN, and NCI-H2347. Cell lines belonging to the pHER3 nondetectable group include: CS1R, LN18, NB69, HuCCT1, DLD-1, DU145, A2.1, NCI-H661, and HSC-2.

(C) Immunoblots showing the effect of acute lapatinib (200 nM) and erlotinib (200 nM) treatment (2 hr) in a panel of lapatinib-sensitive, moderately sensitive, or refractory cell lines on HER3 phosphorylation and downstream AKT phosphorylation.

whether activation of HER3 via the addition of conditioned media to EFM-19 cells requires HER2 kinase activity. Conditioned media from the lapatinib-sensitive cells was added to EFM-19 cells, and cells were cotreated with either lapatinib or erlotinib. As shown in Figure 3C and Figure S3A, cotreatment with lapatinib, but not erlotinib, suppressed HER3 activation in EFM-19 cells. Notably, lapatinib, but not erlotinib, also suppressed HER3 activation in EFM-19 cells treated with conditioned media from KP4, H2722, and HEC-1 lapatinib-refractory cell lines (Figure 3D). Further analysis indicated that the six lapatinib-refractory cell lines that can activate HER3 in the EFM-19 model do not detectably express HER3 protein (Figure 3E), and treatment of KP4, HEC-1, or H2722 cells with lapatinib failed to suppress pAKT (Figure S3B), indicating that AKT signaling is not driven by HER3 in these cells. Collectively, these results suggest that the lapatinib-sensitive cell lines with elevated pHER3 secrete a HER3-activating ligand to engage an autocrine loop to drive cell survival via HER2 kinase activity.

Coexpression of NRG1 and HER3 Associates with Lapatinib Sensitivity

Because the lapatinib-sensitive cell lines all secrete a HER3-activating ligand, we next assessed their expression of the two established HER3 ligands, NRG1 and NRG2. NRG1 protein was significantly elevated in the lapatinib-sensitive lines compared to seven of the lapatinib-refractory lines, whereas no correlation was noted with NRG2 expression (Figure 4A). We also analyzed the expression of NRG1 and NRG2 in a panel of 20 HKI-272-refractory cell lines (also largely refractory to lapatinib; data not shown) as determined from the initial screen (Table S1), with a similar expression profile observed. Of note, all of the lapatinib-sensitive cell lines expressed HER3 protein; whereas the lapatinib-refractory cell lines with elevated NRG1 expression demonstrated undetectable HER3 protein levels. We next determined whether increased NRG1 protein was due to increased mRNA. Overall, we detected relatively high *NRG1* mRNA expression in the lapatinib-sensitive cell lines, with a strong correlation observed between NRG1 protein and mRNA expression (Figure 4B; R^2 = 0.67). Moreover, NRG1 and HER3 coexpression was very strongly correlated with lapatinib sensitivity (Figure 4C; $p < 0.0001$).

To confirm that NRG1 was indeed secreted by the lapatinib-sensitive cells, we analyzed conditioned media from these cells. The nine tested lapatinib-sensitive cell lines all demonstrated detectable NRG1 protein in conditioned media, whereas the lapatinib-refractory EFM-19 and MCF-7 cells, as well as the *HER2*-amplified SKBR3 cell line, showed no detectable expression (Figure 4D). Together, these results indicate that the non-*HER2* amplified lapatinib-sensitive cells secrete NRG1 to activate HER3 in an autocrine manner. Furthermore, elevated expression of NRG1 and HER3 was prominently featured in this lapatinib-sensitive subset of cell lines.

Knockdown of NRG1 Inhibits Cell Proliferation in Lapatinib-Sensitive Cells

To explore the functional relevance of NRG1 in the lapatinib-sensitive cell lines, we performed NRG1 knockdown studies. Four different shRNAs targeting NRG1 successfully decreased NRG1 protein and mRNA (Figure 5A; Figure S4A). Depleting NRG1 in the lapatinib-sensitive cells significantly reduced proliferation, whereas depleting NRG1 in MCF-7 or SKBR3 cells (negative controls) had no detectable effect (Figure 5B; Figure S4B). To control for potential off-target RNAi effects, we carried out a rescue experiment in the lapatinib-sensitive melanoma cell line CHL-1. CHL-1 cells were transduced with shRNAs targeting NRG1 in the presence of recombinant human (rh) NRG1. The addition of rhNRG1 substantially rescued the effects of knocking down NRG1 in CHL-1 cells (Figure 5C). To further confirm that NRG1 was indeed the secreted factor that promoted HER3 activation in these cells, we knocked down NRG1 and tested the ability of these cells to produce conditioned media that activates HER3 in the EFM-19 reporter model. Conditioned media from NRG1-depleted cells failed to activate HER3 in EFM-19 cells compared to shGFP-transduced cells (Figure 5D; Figure S4C). To verify that NRG1 was depleted from the media, we collected and concentrated media from NRG1 shRNA-transduced SN-12C cells. Levels of secreted NRG1 were substantially reduced in cells transduced with shRNAs targeting NRG1 (Figure 5E).

HER2 Kinase Inhibition Suppresses Xenograft Growth in NRG1 Autocrine Cancer Cell Lines

To extend the cell line findings to an in vivo tumor model, we carried out xenograft studies using the FaDu head and neck cancer cell line and the SN-12C renal cell carcinoma cell line. First, to confirm that lapatinib could suppress pHER3 in vivo, we implanted FaDu cells subcutaneously in the flanks of nu/nu mice, and determined that lapatinib treatment (100 mg/kg) effectively suppressed pHER3, as well as pHER2, and pAKT activity in FaDu xenografts (Figure 6A). Next, we assessed the ability of lapatinib to retard tumor growth. Tumors were allowed to grow until they reached an average volume of 130 mm^3 (Figure 6B), at which point mice received either lapatinib or vehicle control every day for 3 weeks. Xenografts of lapatinib-treated mice grew at a significantly slower rate than xenografts of vehicle control-treated mice. Lapatinib also suppressed the growth of SN-12C xenografts, with significant growth only observed once lapatinib treatment was ceased (day 30) (Figure 6C). The modest effects of lapatinib probably reflect its inability to fully suppress pAKT when FaDu cells are grown as xenografts. Consistent with this notion, it was recently reported that intermittent high-dose lapatinib treatment more robustly inhibited HER2 activity compared to standard daily dosing (Amin et al., 2010). To complement the lapatinib findings, and to confirm

(D) Cell viability assay demonstrating suppression of cell proliferation in a panel of lapatinib-sensitive cell lines following lentiviral infection of HER3-specific shRNAs (5 days). MCF-7 cells were used as a negative control for the effects of RNAi. shHER3 475 and shHER3 3293 represent two independent HER3-targeting RNAi sequences, and shGFP is a control vector. On the right are immunoblots showing HER3 protein expression in CHL-1 cells following infection with either a control vector (shGFP) or the HER3-specific shRNAs, 475 and 3293 (72 hr). Error bars represent mean ± SEM.
(E) Immunoblots showing the effect of acute trastuzumab (10 μg/ml), pertuzumab (10 μg/ml), or a HER3-targeted antibody (10 μg/ml) treatment (2 hr) in CHL-1, FaDu, and SAT cells on HER3 phosphorylation and downstream AKT phosphorylation.
(F) Immunoblots showing the expression of EGFR, HER2, pHER3, HER3, pAKT, and AKT in CHL-1 and FaDu cells following infection with two different EGFR, HER2, HER3, or HER4 shRNA vectors (72 hr). shGFP represents a control vector. See also Figure S2.

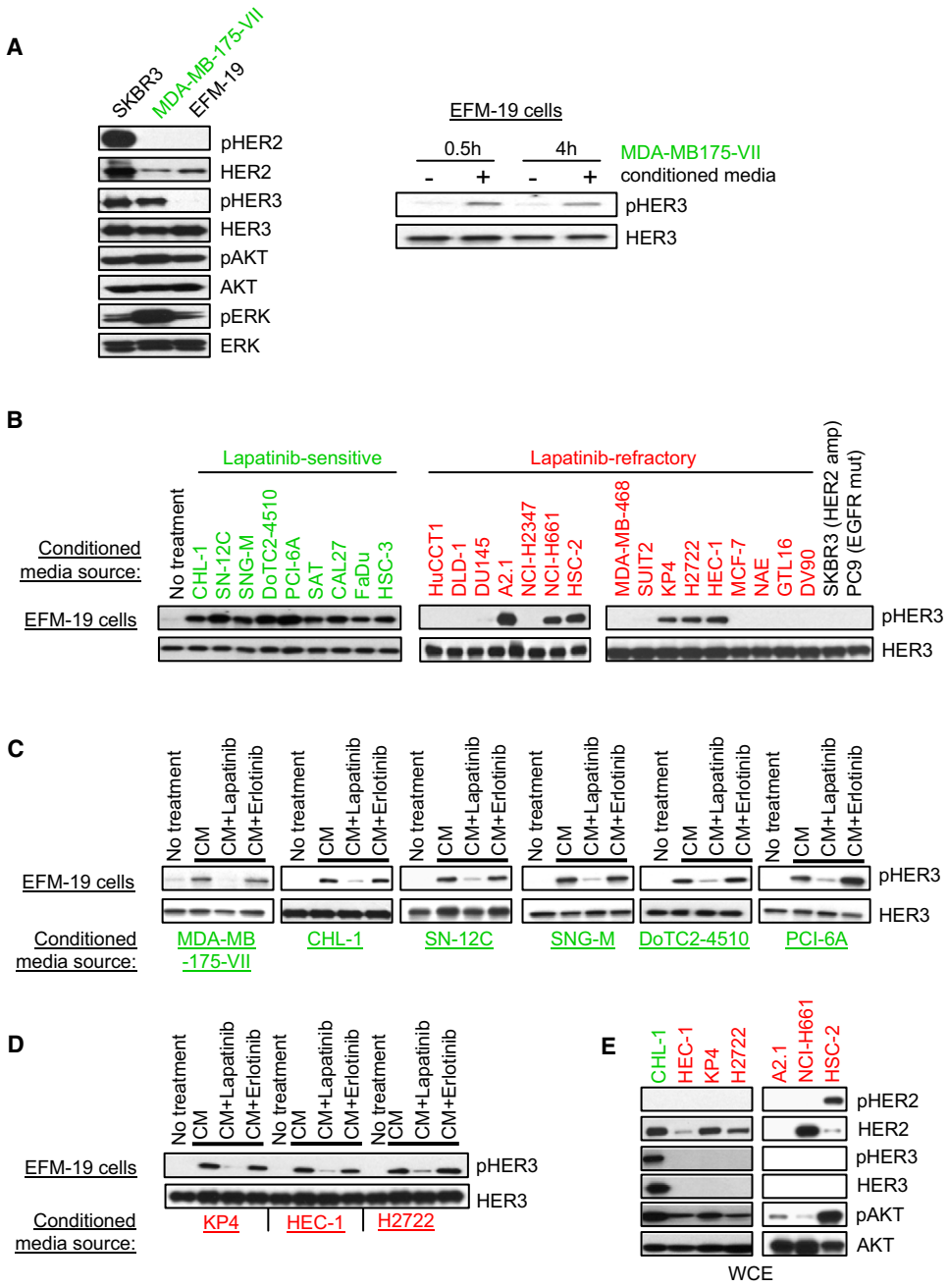

Figure 3. A HER3-Activating Ligand Is Secreted by Non-*HER2* Amplified Lapatinib-Sensitive Cell Lines

(A) Left view has immunoblots showing the expression of pHER2, HER2, pHER3, HER3, pAKT, AKT, pERK, and ERK in the *HER2*-amplified SKBR3, the NRG1-DOC4 fusion containing MDA-MB-175-VII, and the EFM-19 breast cancer cell lines. Right view is of immunoblots demonstrating HER3 activation (pHER3) in EFM-19 cells following the addition of media conditioned overnight from the MDA-MB-175-VII cell line.

(B) Immunoblots showing HER3 activation in EFM-19 cells following the addition of conditioned media (CM) from a panel of lapatinib-sensitive (green) and lapatinib-refractory (red) cell lines (30 min). The effect of conditioned media from the *HER2*-amplified SKBR3 and the *EGFR* mutated PC9 cell lines on the activation of HER3 (pHER3) in EFM-19 cells is also shown.

(C) Immunoblots showing the effects of cotreatment with lapatinib (500 nM) or erlotinib (500 nM) on the ability of CM from the panel of lapatinib-sensitive cell lines to activate HER3 in EFM-19 cells (30 min).

(D) Immunoblots showing the effects of cotreatment with lapatinib (500 nM) or erlotinib (500 nM) on the ability of CM from KP4, HEC-1, and H2722 lapatinib-refractory cell lines to activate HER3 (pHER3) in EFM-19 cells (30 min).

(E) Immunoblots showing the levels of pHER3, HER3, pAKT, and AKT in the lapatinib-refractory KP4, HEC-1, H2722, A2.1, NCI-H661, and HSC-2 cell lines. CHL-1 lysate is included as a positive control for pHER3 levels. WCE, whole-cell extract. See also Figure S3.

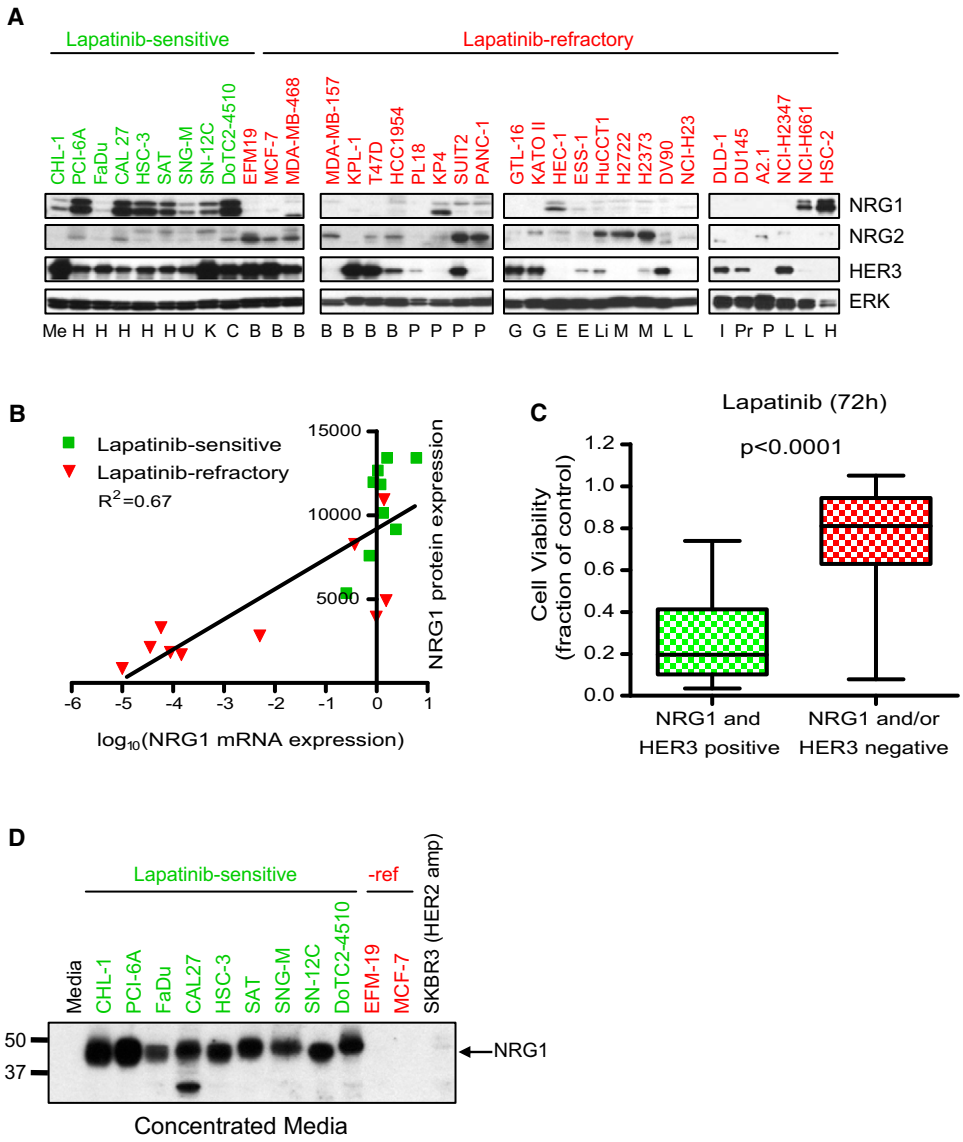

Figure 4. NRG1 Is Highly Expressed and Secreted by the Non-*HER2* Amplified Lapatinib-Sensitive Cell Lines

(A) Immunoblots showing the expression of NRG1, NRG2, HER3, and ERK in the panel of lapatinib-sensitive (green) cell lines and a panel of lapatinib-refractory (red) cell lines derived from multiple tissue types. Cell line histology is indicated below the immunoblots. Me, melanoma; K, kidney; C, cervical; H, head and neck; U, uterus; B, breast; P, pancreatic; G, gastric; E, endometrial; Li, liver; M, mesothelioma; I, intestine; Pr, prostate; L, lung.

(B) Correlation between NRG1 protein and mRNA expression in the panel of lapatinib-sensitive (green squares) and lapatinib-refractory (red triangles) cell lines. Lapatinib-sensitive cell lines include: CHL-1, PCI-6A, FaDu, CAL27, HSC-3, SAT, SNG-M, SN-12C, and DoTC2-4510. Lapatinib-refractory cell lines include: EFM-19, MCF-7, MDA-MB-468, KP4, SUIT2, GTL16, HEC-1, ESS-1, H2722, and DV90.

(C) Box and whisker plot comparing lapatinib response (cell proliferation, 72 hr) in the NRG1 and HER3-coexpressing cells (n = 10) compared to the NRG1 or HER3 negative-expressing cells (n = 21). Statistical difference between the two groups was assessed using Student's t test (two-tailed, $p < 0.0001$).

(D) Immunoblot demonstrating secreted NRG1 in the media from the panel of lapatinib-sensitive cell lines. Media from EFM-19, MCF-7, and SKBR3 cells are included as negative controls.

the suspected role of HER2:HER3 signaling in mediating the tumorigenic properties of these NRG1-driven cells, we also determined that treatment of the xenografted tumors with pertuzumab, a monoclonal antibody that inhibits HER2:HER3 dimerization, similarly suppressed pHER3 as well as tumor growth (Figure 6B). These results support the potential in vivo relevance of the cell culture findings.

Elevated *NRG1* Expression and HER3 Activation in Primary Head and Neck Cancers

To determine the potential clinical relevance of the observed NRG1-mediated autocrine lapatinib sensitivity mechanism, we further explored these biomarker profiles in the setting of head and neck cancer, the most frequently observed tumor type demonstrating lapatinib sensitivity beyond *HER2*-amplified

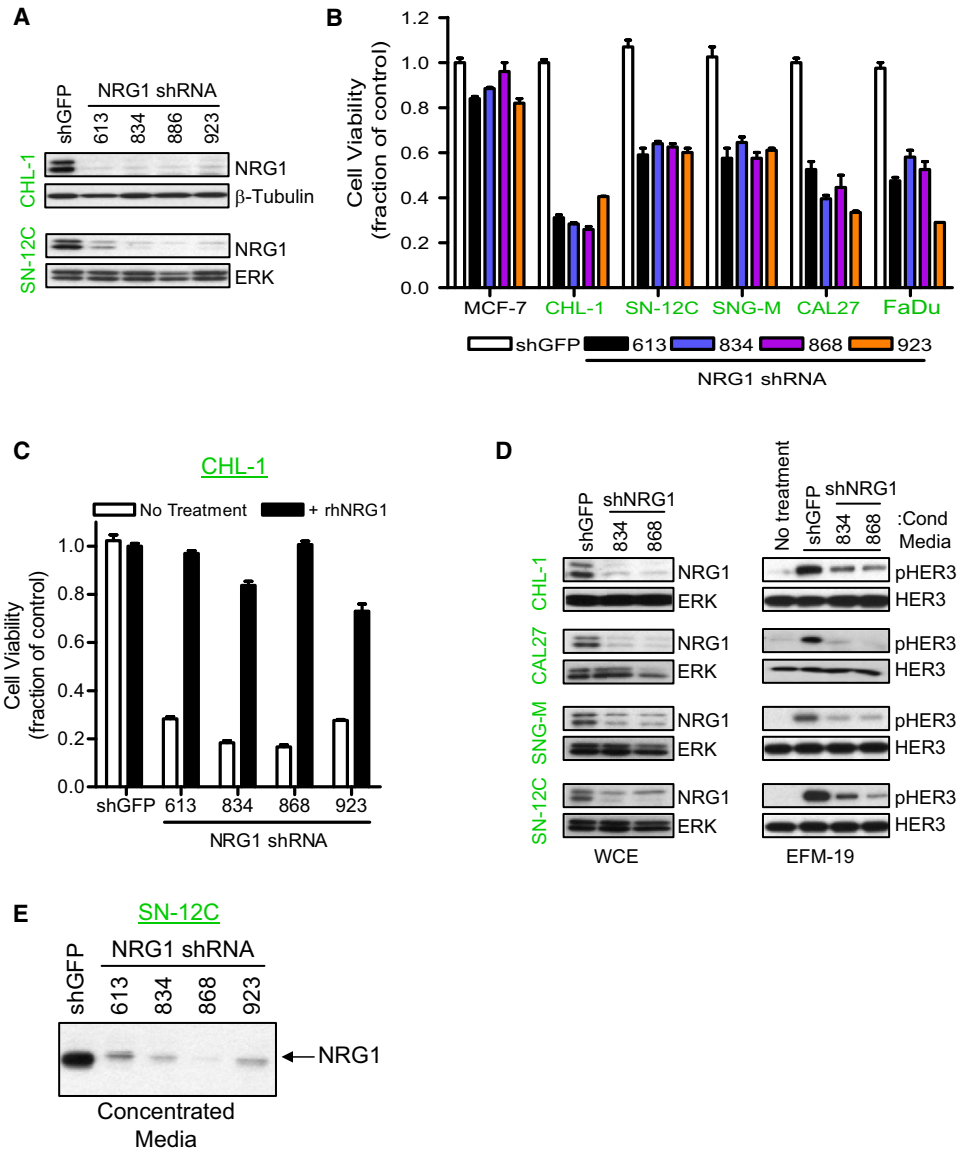

Figure 5. NRG1 Mediates Cell Survival in Non-*HER2* Amplified Lapatinib-Sensitive Cell Lines

(A) Immunoblots showing NRG1 protein expression in CHL-1 and SN-12C cell lines following infection with either a control vector (shGFP) or the NRG1-specific vectors (5 days). The numbers 613, 834, 868, and 923 correspond to four different RNAi sequences.

(B) Cell viability assay demonstrating suppression of cell proliferation in a panel of lapatinib-sensitive cell lines following lentiviral infection of NRG1-specific shRNAs or a control (shGFP) vector (5 days). MCF-7 cells were used to control for the effects of RNAi. Error bars represent mean ± SEM.

(C) Lentiviral rescue experiment in CHL-1 cells transduced with NRG1 shRNAs for 5 days. Following overnight infection, media was changed, and cells were treated daily with rhNRG1-β1 (100 ng/ml) as indicated. Error bars represent mean ± SEM.

(D) Left view has immunoblots showing the expression of NRG1 in a panel of the lapatinib-sensitive cell lines following infection with either a control (shGFP) or NRG1 (834 and 868) shRNA vectors (5 days). WCE, whole-cell extract. Right view is of immunoblots showing the activation of HER3 (pHER3) in EFM-19 cells following the addition of conditioned media from the panel of lapatinib-sensitive cells on the left (30 min). Twenty-four hours prior, lentiviral-infected cells were washed, and the media was replaced with unsupplemented media. The volume of conditioned media added to EFM-19 cells was adjusted to control for the antiproliferative effect observed in the NRG1 shRNA-transduced cells.

(E) Detection of secreted NRG1 in the media from SN-12C cells following lentiviral infection with a control vector (shGFP) or 4 different NRG1 shRNAs; 613, 834, 868, and 923 (5 days). Twenty-four hours prior to collection, the cells were washed and the media replaced with unsupplemented media. See also Figure S4.

breast cancers. Initially, we compared levels of pHER3 and NRG1 between the five lapatinib-sensitive head and neck caner cell lines previously described (Figures 2A and 4A) and a set of five lapatinib-refractory head and neck cancer cell lines that failed to respond to HKI-272 (Table S1 and Figure S5A). Similar to our previous findings, elevated NRG1 expression and increased pHER3 were observed in the panel of head and neck cancer-derived lapatinib-sensitive cell lines (Figure 7A). Significantly, NRG1 expression and pHER3 were undetectable in the panel of lapatinib-refractory head and neck cancer cell

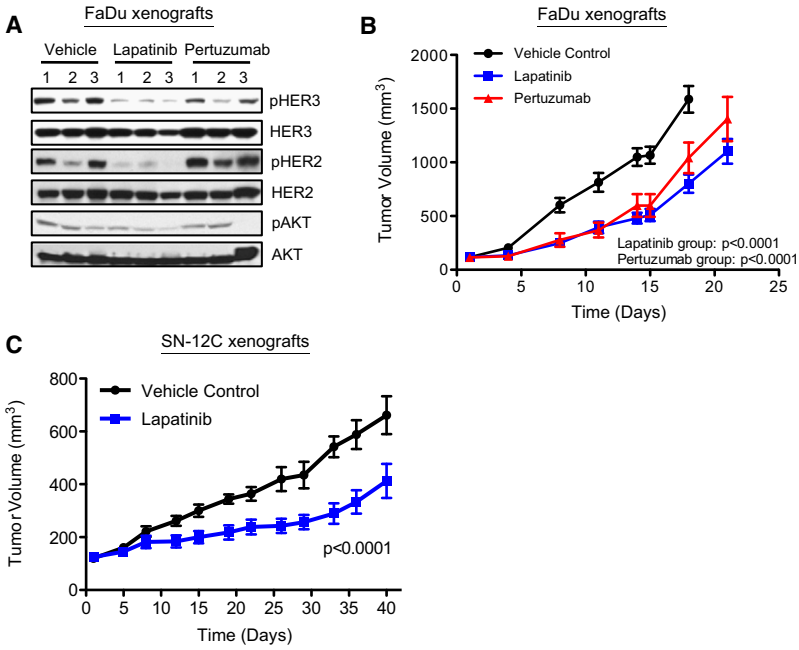

Figure 6. HER2 Kinase Inhibition Retards the Growth of NRG1-Driven Tumor Cells In Vivo

(A) Immunoblots showing suppression of pHER3, pHER2, and pAKT in FaDu xenografts following treatment with either lapatinib or pertuzumab.

(B) Tumor growth assay showing the antitumor effect of lapatinib and pertuzumab on FaDu xenografts. Mice were treated as stated in the Experimental Procedures. Differences between the lapatinib or pertuzumab-treated group and the vehicle control-treated group were calculated using two-way ANOVA. Error bars represent mean ± SEM.

(C) Tumor growth assay showing the antitumor effect of lapatinib on SN-12C xenografts. Mice were treated as stated in the Experimental Procedures. Differences between the two groups were calculated using two-way ANOVA. Error bars represent mean ± SEM.

lines. Moreover, NRG1 was undetectable in the conditioned media of the lapatinib-refractory cell lines (Figure S5B). Consistent with the findings described above, we found that elevated *NRG1*, but not *HER3*, mRNA expression correlated with lapatinib response (Figure 7B; Figure S5C). Biochemically, lapatinib (or erlotinib) failed to suppress pAKT in the lapatinib-refractory head and neck cancer cell lines, indicating that the HER2 kinase is not signaling to AKT in these cell lines (Figure S5D).

Next, we assessed *NRG1* and *HER3* mRNA levels in 29 primary head and neck cancer samples and compared the expression to the lapatinib-sensitive cell lines and a panel of 17 lapatinib-refractory cell lines (Figure 7C). All of the lapatinib-sensitive cell lines demonstrated relatively high levels of *NRG1* mRNA expression, with coexpression of *HER3* mRNA (Figure 7C). Of note, *NRG1* mRNA expression was nearly undetectable in 12 out of 17 lapatinib-refractory cell lines. Elevated *NRG1* mRNA expression was also observed in KP4 and HEC-1 lapatinib-refractory cell lines, which correlated with NRG1 protein expression (Figure 4A). However, elevated *NRG1* mRNA expression was also observed in the ESS-1 endometrial cancer and H2722 mesothelioma cell lines, which failed to correlate with increased NRG1 protein expression (Figure 4A), indicating that NRG1 expression may be regulated at the post-transcriptional level in these cells. Similar to what was observed at the HER3 protein level (Figure 4A), the lapatinib-refractory, *NRG1*-elevated cell lines displayed low levels of *HER3* mRNA. Significantly, we found that 12 out of 29 primary tumor samples displayed similar elevated levels of *NRG1* and coexpression of *HER3* (Figure 7C). Strikingly, 6 primary tumor samples (13, 17, 22, 24, 25, and 29) showed extremely high expression levels of *NRG1* mRNA as compared to the expression observed in the lapatinib-sensitive cell lines. Of note, this biomarker profile was not observed in primary lung cancer samples, where *NRG1* mRNA was barely detectable in the majority of cases (Figure S5E). We also carried out an immunoprecipitation (IP)-immunoblot to determine if the HER3 receptor was detectably activated in the primary tumor samples. Significantly, we detected pHER3 in four of ten samples analyzed (Figure 7D). Importantly, these four samples (out of five) in this subset analyzed, displayed at least median expression of *NRG1* mRNA. Collectively, these data indicate that a significant proportion of head and neck tumors may exhibit a dependency on a NRG1-mediated autocrine loop, and could consequently respond to HER2:HER3-targeted therapies.

DISCUSSION

The ability to predict a cancer patient's response to drug treatment based on specific molecular features of their tumor cells is beginning to dramatically impact the practice of medical oncology. Thus, the identification of predictive biomarkers in the form of "drug-sensitizing" oncogenic alleles such as fusion genes (*BCR-ABL* and *EML4-ALK*), activating mutations (*EGFR* and *BRAF*), or genomic amplification (*HER2*) has been critical to the successful clinical development of molecularly targeted drugs that are selectively efficacious in these genomically defined patient subsets (Sharma and Settleman, 2007). At the same time, many of these drug targets—the kinases in particular—may contribute to tumorigenesis despite the absence of target-associated genomic lesions, possibly pointing to additional settings in which these same drugs could be clinically effective. Here, we observed that HER2-directed kinase inhibitors may be effective antitumor agents beyond the context of *HER2* gene amplification, the only clinical setting in which they are currently employed. We determined that a subset of a very large panel of tested human cancer cells lines, derived from multiple tissue types, exhibits a strict dependence on NRG1 secretion that drives HER2:HER3-mediated downstream survival signals. Of note, this autocrine survival mechanism was most frequently observed in head and neck carcinomas. In addition this subset of drug-sensitive cell lines, which do not exhibit *EGFR* or *HER2* genomic activation, was defined by elevated NRG1 expression, as well as coexpression of HER3, a biomarker observed in a significant subset of primary head and neck tumors. These findings suggest that a molecularly defined

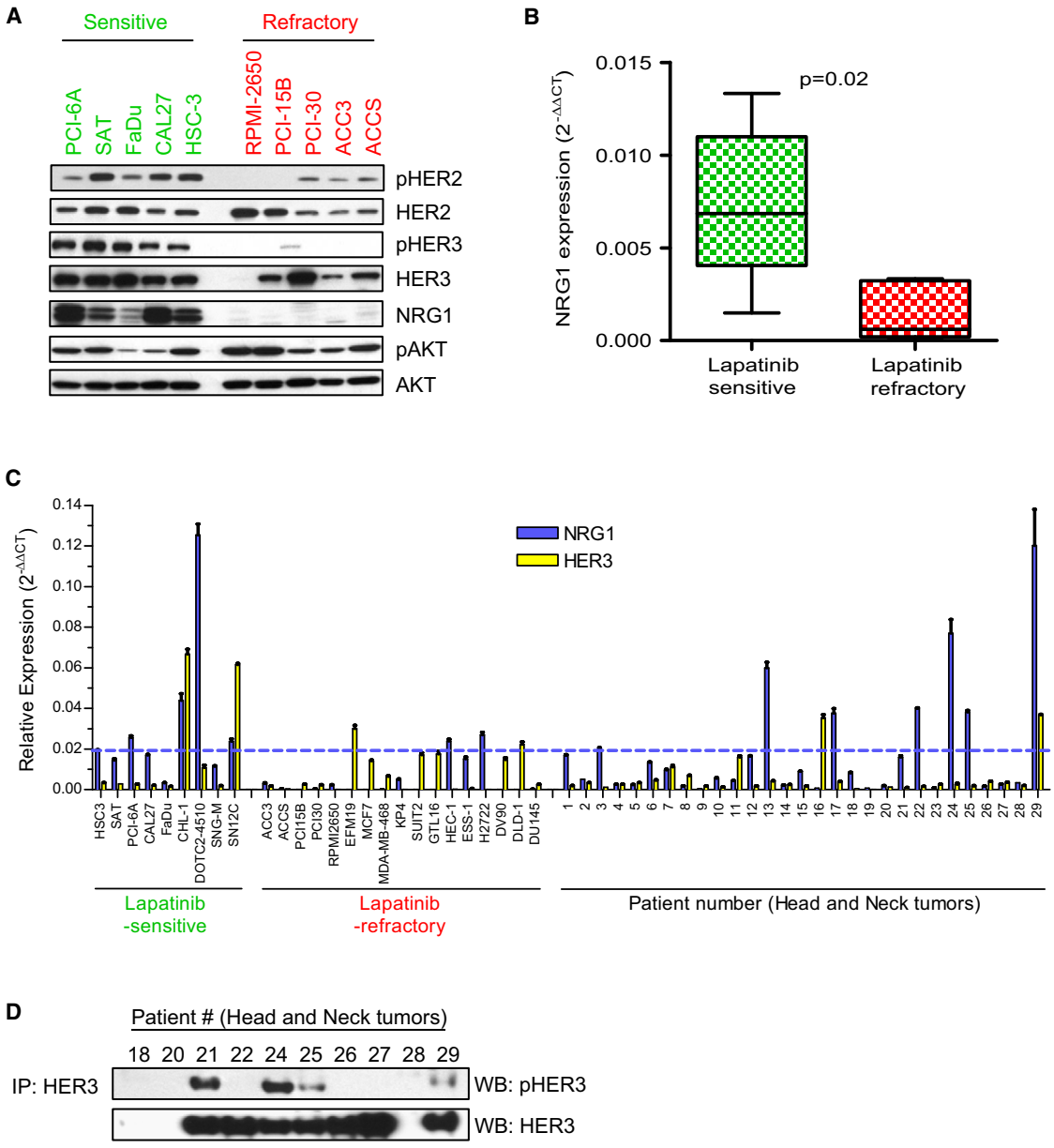

Figure 7. A Lapatinib Sensitivity Biomarker Is Observed in Head and Neck Primary Tumors

(A) Immunoblots showing the levels of pHER2, HER2, pHER3, HER3, NRG1, pAKT, and AKT in a panel of lapatinib-sensitive and -refractory head and neck tumor-derived cell lines.

(B) Box and whisker plot comparing *NRG1* mRNA expression between the lapatinib-sensitive and lapatinib-refractory head and neck cancer cell lines. Statistical difference between the two groups was assessed using Student's t test (two-tailed, $p = 0.026$).

(C) Quantitative PCR analysis showing the expression of *NRG1* and *HER3* in head and neck primary tumor samples. As a comparison for expression, lapatinib-sensitive and -refractory cell lines are included. The blue dashed line represents the median *NRG1* expression calculated using the expression from the panel of lapatinib-sensitive cell lines. Error bars represent mean ± SEM.

(D) Immunoblot showing the constitutive activation of HER3 (pHER3) in a subset of head and neck primary tumor samples. HER3 was immunoprecipitated as described in the Experimental Procedures and subsequently immunoblotted with antibodies directed against pHER3 and HER3, respectively. See also Figure S5.

subset of cancer patients lacking *HER2* gene amplification may benefit from therapy with HER2:HER3-targeted drugs.

Following the clinical success of cetuximab in the treatment of metastatic head and neck cancer patients, early-phase studies to assess the potential benefit of lapatinib treatment have recently been initiated. In a phase I study, lapatinib in combination with chemoradiation revealed an acceptable tolerability profile, with an objective response rate of 81% observed (Harrington et al., 2009). In a phase II study, prolonged tumor stabilization was observed in 36% of patients with malignant salivary gland tumors (Agulnik et al., 2007). However, in this study only patients whose tumor stained 2+ for HER2 by IHC were included.

Unfortunately, such studies would not be expected to reveal potential clinical activity in patients whose tumors are driven by NRG1-mediated autocrine signaling, as would be anticipated based on our preclinical findings. Another phase I study assessing lapatinib toxicity in patients with solid malignancies demonstrated stable disease in 29% of patients, with one patient experiencing a complete response (Burris et al., 2009). These results are consistent with a role for HER2 kinase inhibition beyond the context of *HER2*-amplified breast cancer.

The oncogenic RTKs can all potentially be engaged via elevated expression of their associated ligands, either produced by tumor stroma or the tumor cells themselves. Such paracrine or autocrine activation of these receptors, which may be expressed at relatively low levels on tumor cells, is likely to go undetected by traditional techniques used to measure receptor expression or by assessing common receptor-activating mutations that have been found in various tumor types. Our findings demonstrate that a HER2-mediated autocrine loop drives a subset of NRG1-overexpressing tumors and may be relevant to other RTK-mediated oncogenic pathways. We have previously reported a PDGF (platelet-derived growth factor)-driven NSCLC cell line that demonstrated striking sensitivity to the PDGFR TKI sunitinib (McDermott et al., 2009). Similarly, treatment of the KP4 HGF-secreting orthotopic model of pancreatic cancer with a monoclonal antibody targeting Met (MetMAb) retarded xenograft growth resulting in a substantial survival benefit (Jin et al., 2008). Further clinical studies are warranted to substantiate these preclinical observations.

The dynamic range of *NRG1* mRNA expression observed in the cell line models and tumor samples we analyzed potentially reflects the contribution of both genetic and epigenetic regulatory mechanisms. To date, mutational activation of NRG1 has only been documented in a single example—the NRG1-DOC4 fusion protein, resulting from chromosomal translocation, discovered in the MDA-MB-175VII breast cancer cell line (Schaefer et al., 1997). Of note, the 8p chromosomal arm, where the *NRG1* gene resides, has been shown to undergo rearrangements in a significant proportion of breast cancer cell lines (Huang et al., 2004; Pole et al., 2006). In addition chromosomal breaks within this region were discovered in 6% of primary breast tumors, the majority of which were HER2-low tumors. The functional significance of the potential fusion proteins observed in these studies has yet to be demonstrated but highlights the potentially complex nature of *NRG1* mRNA regulation. In addition methylation of the *NRG1* transcriptional promoter site has also been shown to negatively regulate mRNA expression in breast cancer cell lines, with a correlation noted in primary tumor samples (Chua et al., 2009). This may also explain the differences we observed in our cell line models and tumor samples.

Expression of the EGFR family ligands has been well established in certain epithelial-derived cancers, especially those derived from the colon, breast, lung, and ovary (Normanno et al., 2006; Yotsumoto et al., 2009). The HER family of ligands, including EGF, transforming growth factor α, amphiregulin, betacellulin, heparin-binding-EGF, and NRG1, has been previously shown to be expressed to various levels in a panel of head and neck cancer cell lines (O-Charoenrat et al., 2000; O-Charoenrat et al., 2002). In those studies treatment with exogenous HER family ligands led to an increase in mRNA expression of the corresponding ligand-encoding genes, most notably for heparin-binding EGF and NRG1, implicating an autocrine induction of ligand. In addition Yonesaka et al. (2008) demonstrated that autocrine production of amphiregulin in EGFR wild-type lung and head and neck cancer cell lines is associated with sensitivity to cetuximab. These results present further possible therapeutic strategies to inhibit NRG1, and other EGFR ligand-mediated autocrine signals. Thus, neutralizing antibodies that disrupt ligand binding may be efficacious at multiple levels in inhibiting the autocrine signal.

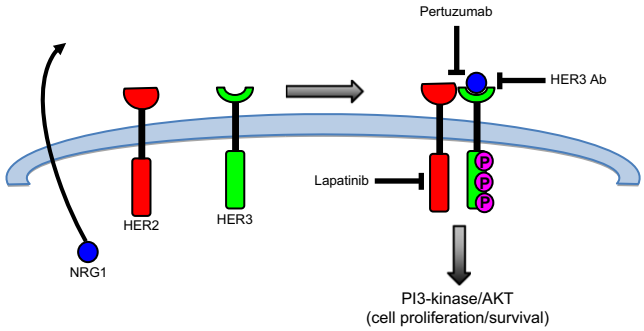

Figure 8. Model Depicting the Proposed NRG1-Mediated Autocrine-Signaling Mechanism

NRG1 secreted by cancer cells in an autocrine manner binds to HER3, resulting in its heterodimerization with HER2. HER2 subsequently phosphorylates HER3 resulting in the activation of the PI3K/AKT pathway promoting cell survival and proliferation. Importantly, transphosphorylation of HER2 is not required for this signaling cascade. As proposed, this pathway can be inhibited at multiple steps: first, by preventing NRG1 from binding HER3 using HER3-targeted antibodies; second, by preventing HER2:HER3 heterodimerization using a heterodimer-blocking antibody, such as pertuzumab; and finally, by inhibiting HER2 kinase activity using a HER2 TKI such as lapatinib.

In summary our findings suggest that a patient subpopulation defined by elevated *NRG1* expression, and coexpression and activation of HER3, may derive clinical benefit from HER2:HER3-targeted therapies such as lapatinib (Figure 8). Thus, the initiation of a clinical trial in a genomically defined patient subset, most probably in the setting of head and neck carcinoma, is warranted to assess these preclinical findings. The observations also highlight the potential importance of identifying nonmutationally driven RTK dependencies in human tumors to inform biomarker strategies for clinical development of selective kinase inhibitors.

EXPERIMENTAL PROCEDURES

Human Cancer Cell Lines and High-Throughput Tumor Cell Line Screening

Human cancer cell lines were obtained and tested for sensitivity using an automated platform as previously described (McDermott et al., 2007). Cell lines were maintained at 37°C in a humidified atmosphere at 5% CO_2 and grown in RPMI 1640 or DMEM/F12 growth media (GIBCO) supplemented with 10% fetal bovine serum (GIBCO), 50 U/ml penicillin, and 50 μg/ml streptomycin (GIBCO).

Cell Viability Assays

Cell viability was assessed using the nucleic acid stain SYTO 60 (Invitrogen). Cells (3000 per well) were seeded into 96-well plates, allowed to adhere overnight, and exposed to a range of drug concentrations. After 72 hr, cells were fixed in 4% formaldehyde, stained with SYTO 60, and cell viability was

assessed by fluorescence measurement using a SpectraMax M5 microplate reader (excitation 630 nm, emission 695 nm; Molecular Devices). The fraction of control was calculated by dividing the fluorescence obtained from the drug-treated cells by the fluorescence obtained from the control (no drug)-treated cells.

Reagents

HKI-272 was obtained from Wyeth Pharmaceuticals. Lapatinib and erlotinib were purchased from LC Laboratories. rhNRG1-β1 was purchased from R&D Systems. Pertuzumab, trastuzumab, and the HER3-targeted antibody were produced at Genentech. The HER3-directed antibody was selected from a human phage-displayed antibody library with synthetic diversity in the selected complementarity determining regions. It was obtained by panning on immobilized HER3 ECD (HER3-ECD-Fc fusion protein comprising amino acids 1–621 fused to the Fc domain of human IgG) as described previously (Lee et al., 2004). The antibody blocks the binding of ligand (NRG1) to HER3.

Immunoblotting

Cell lysates were harvested using Nonidet-P40 lysis buffer, supplemented with Halt protease and phosphatase inhibitor cocktail (Thermo Scientific), and immunodetection of proteins was carried out using standard protocols. The phospho-EGFR (#2236), phospho-HER2 (#2247), HER2 (#2242), phospho-HER3 (Y1289; #4791), AKT (#9272), phospho-ERK (T202/Y204; #9101), ERK (#9102), and HER4 (#4795) antibodies were purchased from Cell Signaling Technology. Antibodies to HER3 (SC-285), NRG1 (SC-28916), NRG2 (SC-67001), and EGFR (SC-03) were purchased from Santa Cruz Biotechnology. Phospho-AKT (S473; #44-621G) antibody was purchased from Invitrogen. GAPDH (MAB374) antibody was purchased from Chemicon. Densitometry was carried out using ImageJ software.

Detection of Secreted NRG1

Cells were grown to approximately 80% confluency on a 10 cm dish in normal growth media, washed once in PBS, and serum starved in 10 ml unsupplemented RPMI 1640 or DMEM/F12 growth media as appropriate. Following overnight incubation, media was harvested, and cell debris was pelleted at 1500 rpm for 5 min. The conditioned media was then concentrated using Millipore Amicon Ultra (3K) centrifugal filters at 4000 × g for 40 min. The concentrate was transferred to a 1.5 ml ultracentrifuge tube, and one-third the volume of 4× Sample buffer was added and boiled at 95°C for 5 min to denature any proteins. A total of 20 μl of sample was immunoblotted using standard techniques. Secreted NRG1 was detected using MAB377 monoclonal antibody from R&D Systems.

Lentiviral shRNA Studies

shRNA constructs were obtained from the Broad RNAi consortium, and the sequences are shown in Supplemental Experimental Procedures. Lentivirus production was carried out in 293T cells as previously described (Moffat et al., 2006). For knockdown studies cells were plated in 96-well (3000 cells per well) or 6-well dishes (2×10^5 cells per well). Following adherence overnight, cells were spin infected with lentivirus or control virus in the presence of polybrene (hexadimethrine bromide; Sigma-Aldrich) at 1200 × g for 75 min at 32°C. Twenty-four hours postinfection, media was replaced with regular growth media. Depending on the experiment, cells were harvested 3 or 5 days post-lentiviral infection for protein lysates, RNA lysates, or cell viability, which was assayed using SYTO 60 nucleic acid stain as described.

Quantitative PCR Analysis

RNA was extracted from cells using the RNeasy kit (QIAGEN), and 1 μg RNA was reverse transcribed using the high-capacity RNA-to-cDNA kit (Applied Biosystems) according to manufacturer's instructions. The amount of amplicon was determined using the Applied Biosystems 7500 quantitative PCR system using SYBR green as the fluorescence reporter. Each sample was normalized to the housekeeping gene GAPDH. All samples were analyzed in triplicate, and the relative expression was determined. Primer sequences are listed in Supplemental Experimental Procedures.

Xenograft Studies

All procedures involving animals were approved by Piedmont's Research Center's Institutional Animal Care and Use Committee (IACUC) and carried out in an AAALAC (Association for the Assessment and Accreditation of Laboratory Animal Care) accredited facility. FaDu tumor xenografts were grown in athymic nude mice from Harlan (nu/nu). On the day of implantation, 5×10^6 FaDu cells were injected subcutaneously into the flank of 8-week-old mice. Tumors were allowed to grow until they reached a size of 88–172 mm^3, at which point mice were randomized into three groups of ten mice each. One group of animals was treated by oral gavage with lapatinib at 100 mg/kg for 21 days. A second group of animals was treated by intraperitoneal injection with pertuzumab at 50 mg/kg on day 0 and 25 mg/kg on days 7 and 14. The final group of animals was treated with vehicles of both agents. An additional three animals per group were treated for 2 days and then sacrificed for tumor collection. For the SN-12C xenograft model, 1×10^7 SN-12C cells were injected subcutaneously into the flank of 8-week-old mice, and tumors were allowed to grow until they reached a size of 108–196 mm^3. Mice were randomized into two groups of eight mice each, with one group of animals receiving lapatinib (100 mg/kg) by oral gavage for 30 days, and the other group receiving vehicle control. Tumor sizes and body weights were measured twice weekly over the course of treatment.

Tissue Samples

Primary human tumor samples with appropriate IRB approval and patient-informed consent were obtained from commercial sources. The human tissue samples used in the study were deidentified (double coded) prior to their use, and hence, the study using these samples is not considered human subject research under the U.S. Department of Human and Health Services regulations and related guidance (45 CFR, Part 46). The head and neck squamous cell carcinoma tumors were from Asterand. The NSCLC tumor specimens, which were adenocarcinomas, were from Asterand and ProteoGenex. For RNA extraction, tissue sections were submerged in 300 ml RLT buffer (QIAGEN) and homogenized using a handheld homogenizer (Polytron) and extracted using TRIzol (Invitrogen), as per the manufacturer's instructions. cDNA was generated using the High-Capacity Reverse Transcription Kit (Applied Biosystems). For IP, 2 mg of NP-40 lysed tissue sample was incubated overnight with 5 μg HER3 antibody and protein G. After three washes, the samples were eluted with western sample buffer, boiled at 95°C for 5 min, and immunoblotted as described above.

Statistical Analysis

Box and whisker plots were carried out to compare the differences between two groups of cell lines. The line indicates the median value, the box represents the upper and lower quartile, and the whiskers represent the lowest and highest value. Differences between the two groups were determined using Student's t test.

SUPPLEMENTAL INFORMATION

Supplemental Information includes Supplemental Experimental Procedures, five figures, and two tables and can be found with this article online at doi:10.1016/j.ccr.2011.07.011.

ACKNOWLEDGMENTS

We thank Toshi Shioda for lentiviral shRNA constructs, and members of the Settleman laboratory for helpful discussions. We also thank Jeff Engelman and his laboratory members for advice throughout the course of these studies. We thank Gabriele Schaefer and Germaine Fuh for providing the HER3-targeted antibody. J.S., D.S.S., and L.B. are employees of Genentech and shareholders of Roche, Inc. T.R.W. is an employee of Genentech.

Received: March 10, 2011
Revised: June 19, 2011
Accepted: July 21, 2011
Published: August 15, 2011

REFERENCES

Agulnik, M., Cohen, E.W., Cohen, R.B., Chen, E.X., Vokes, E.E., Hotte, S.J., Winquist, E., Laurie, S., Hayes, D.N., Dancey, J.E., et al. (2007). Phase II study of lapatinib in recurrent or metastatic epidermal growth factor receptor and/or erbB2 expressing adenoid cystic carcinoma and non adenoid cystic carcinoma malignant tumors of the salivary glands. J. Clin. Oncol. *25*, 3978–3984.

Amin, D.N., Sergina, N., Ahuja, D., McMahon, M., Blair, J.A., Wang, D., Hann, B., Koch, K.M., Shokat, K.M., and Moasser, M.M. (2010). Resiliency and vulnerability in the HER2-HER3 tumorigenic driver. Sci. Transl. Med. *2*, 16ra17.

Bantscheff, M., Eberhard, D., Abraham, Y., Bastuck, S., Boesche, M., Hobson, S., Mathieson, T., Perrin, J., Raida, M., Rau, C., et al. (2007). Quantitative chemical proteomics reveals mechanisms of action of clinical ABL kinase inhibitors. Nat. Biotechnol. *25*, 1035–1044.

Berger, M.B., Mendrola, J.M., and Lemmon, M.A. (2004). ErbB3/HER3 does not homodimerize upon neuregulin binding at the cell surface. FEBS Lett. *569*, 332–336.

Bose, R., and Zhang, X. (2009). The ErbB kinase domain: structural perspectives into kinase activation and inhibition. Exp. Cell Res. *315*, 649–658.

Burris, H.A., 3rd, Taylor, C.W., Jones, S.F., Koch, K.M., Versola, M.J., Arya, N., Fleming, R.A., Smith, D.A., Pandite, L., Spector, N., and Wilding, G. (2009). A phase I and pharmacokinetic study of oral lapatinib administered once or twice daily in patients with solid malignancies. Clin. Cancer Res. *15*, 6702–6708.

Chua, Y.L., Ito, Y., Pole, J.C., Newman, S., Chin, S.F., Stein, R.C., Ellis, I.O., Caldas, C., O'Hare, M.J., Murrell, A., and Edwards, P.A. (2009). The NRG1 gene is frequently silenced by methylation in breast cancers and is a strong candidate for the 8p tumour suppressor gene. Oncogene *28*, 4041–4052.

Garrett, T.P., McKern, N.M., Lou, M., Elleman, T.C., Adams, T.E., Lovrecz, G.O., Kofler, M., Jorissen, R.N., Nice, E.C., Burgess, A.W., and Ward, C.W. (2003). The crystal structure of a truncated ErbB2 ectodomain reveals an active conformation, poised to interact with other ErbB receptors. Mol. Cell *11*, 495–505.

Harrington, K.J., El-Hariry, I.A., Holford, C.S., Lusinchi, A., Nutting, C.M., Rosine, D., Tanay, M., Deutsch, E., Matthews, J., D'Ambrosio, C., et al. (2009). Phase I study of lapatinib in combination with chemoradiation in patients with locally advanced squamous cell carcinoma of the head and neck. J. Clin. Oncol. *27*, 1100–1107.

Holbro, T., and Hynes, N.E. (2004). ErbB receptors: directing key signaling networks throughout life. Annu. Rev. Pharmacol. Toxicol. *44*, 195–217.

Huang, H.E., Chin, S.F., Ginestier, C., Bardou, V.J., Adélaïde, J., Iyer, N.G., Garcia, M.J., Pole, J.C., Callagy, G.M., Hewitt, S.M., et al. (2004). A recurrent chromosome breakpoint in breast cancer at the NRG1/neuregulin 1/heregulin gene. Cancer Res. *64*, 6840–6844.

Hynes, N.E., and Lane, H.A. (2005). ERBB receptors and cancer: the complexity of targeted inhibitors. Nat. Rev. Cancer *5*, 341–354.

Jin, H., Yang, R., Zheng, Z., Romero, M., Ross, J., Bou-Reslan, H., Carano, R.A., Kasman, I., Mai, E., Young, J., et al. (2008). MetMAb, the one-armed 5D5 anti-c-Met antibody, inhibits orthotopic pancreatic tumor growth and improves survival. Cancer Res. *68*, 4360–4368.

Kwak, E.L., Bang, Y.J., Camidge, D.R., Shaw, A.T., Solomon, B., Maki, R.G., Ou, S.H., Dezube, B.J., Jänne, P.A., Costa, D.B., et al. (2010). Anaplastic lymphoma kinase inhibition in non-small-cell lung cancer. N. Engl. J. Med. *363*, 1693–1703.

Lee, C.V., Liang, W.C., Dennis, M.S., Eigenbrot, C., Sidhu, S.S., and Fuh, G. (2004). High-affinity human antibodies from phage-displayed synthetic Fab libraries with a single framework scaffold. J. Mol. Biol. *340*, 1073–1093.

Lee-Hoeflich, S.T., Crocker, L., Yao, E., Pham, T., Munroe, X., Hoeflich, K.P., Sliwkowski, M.X., and Stern, H.M. (2008). A central role for HER3 in HER2-amplified breast cancer: implications for targeted therapy. Cancer Res. *68*, 5878–5887.

McDermott, U., Sharma, S.V., Dowell, L., Greninger, P., Montagut, C., Lamb, J., Archibald, H., Raudales, R., Tam, A., Lee, D., et al. (2007). Identification of genotype-correlated sensitivity to selective kinase inhibitors by using high-throughput tumor cell line profiling. Proc. Natl. Acad. Sci. USA *104*, 19936–19941.

McDermott, U., Iafrate, A.J., Gray, N.S., Shioda, T., Classon, M., Maheswaran, S., Zhou, W., Choi, H.G., Smith, S.L., Dowell, L., et al. (2008). Genomic alterations of anaplastic lymphoma kinase may sensitize tumors to anaplastic lymphoma kinase inhibitors. Cancer Res. *68*, 3389–3395.

McDermott, U., Ames, R.Y., Iafrate, A.J., Maheswaran, S., Stubbs, H., Greninger, P., McCutcheon, K., Milano, R., Tam, A., Lee, D.Y., et al. (2009). Ligand-dependent platelet-derived growth factor receptor (PDGFR)-alpha activation sensitizes rare lung cancer and sarcoma cells to PDGFR kinase inhibitors. Cancer Res. *69*, 3937–3946.

Medina, P.J., and Goodin, S. (2008). Lapatinib: a dual inhibitor of human epidermal growth factor receptor tyrosine kinases. Clin. Ther. *30*, 1426–1447.

Moffat, J., Grueneberg, D.A., Yang, X., Kim, S.Y., Kloepfer, A.M., Hinkle, G., Piqani, B., Eisenhaure, T.M., Luo, B., Grenier, J.K., et al. (2006). A lentiviral RNAi library for human and mouse genes applied to an arrayed viral high-content screen. Cell *124*, 1283–1298.

Normanno, N., De Luca, A., Bianco, C., Strizzi, L., Mancino, M., Maiello, M.R., Carotenuto, A., De Feo, G., Caponigro, F., and Salomon, D.S. (2006). Epidermal growth factor receptor (EGFR) signaling in cancer. Gene *366*, 2–16.

O-Charoenrat, P., Rhys-Evans, P., and Eccles, S. (2000). Expression and regulation of c-ERBB ligands in human head and neck squamous carcinoma cells. Int. J. Cancer *88*, 759–765.

O-Charoenrat, P., Rhys-Evans, P.H., Modjtahedi, H., and Eccles, S.A. (2002). The role of c-erbB receptors and ligands in head and neck squamous cell carcinoma. Oral Oncol. *38*, 627–640.

Pole, J.C., Courtay-Cahen, C., Garcia, M.J., Blood, K.A., Cooke, S.L., Alsop, A.E., Tse, D.M., Caldas, C., and Edwards, P.A. (2006). High-resolution analysis of chromosome rearrangements on 8p in breast, colon and pancreatic cancer reveals a complex pattern of loss, gain and translocation. Oncogene *25*, 5693–5706.

Salomon, D.S., Brandt, R., Ciardiello, F., and Normanno, N. (1995). Epidermal growth factor-related peptides and their receptors in human malignancies. Crit. Rev. Oncol. Hematol. *19*, 183–232.

Schaefer, G., Fitzpatrick, V.D., and Sliwkowski, M.X. (1997). Gamma-heregulin: a novel heregulin isoform that is an autocrine growth factor for the human breast cancer cell line, MDA-MB-175. Oncogene *15*, 1385–1394.

Sequist, L.V., and Lynch, T.J. (2008). EGFR tyrosine kinase inhibitors in lung cancer: an evolving story. Annu. Rev. Med. *59*, 429–442.

Sharma, S.V., and Settleman, J. (2007). Oncogene addiction: setting the stage for molecularly targeted cancer therapy. Genes Dev. *21*, 3214–3231.

Sharma, S.V., Haber, D.A., and Settleman, J. (2010). Cell line-based platforms to evaluate the therapeutic efficacy of candidate anticancer agents. Nat. Rev. Cancer *10*, 241–253.

Sheng, Q., Liu, X., Fleming, E., Yuan, K., Piao, H., Chen, J., Moustafa, Z., Thomas, R.K., Greulich, H., Schinzel, A., et al. (2010). An activated ErbB3/NRG1 autocrine loop supports in vivo proliferation in ovarian cancer cells. Cancer Cell *17*, 298–310.

Shi, F., Telesco, S.E., Liu, Y., Radhakrishnan, R., and Lemmon, M.A. (2010). ErbB3/HER3 intracellular domain is competent to bind ATP and catalyze autophosphorylation. Proc. Natl. Acad. Sci. USA *107*, 7692–7697.

Slamon, D.J., Leyland-Jones, B., Shak, S., Fuchs, H., Paton, V., Bajamonde, A., Fleming, T., Eiermann, W., Wolter, J., Pegram, M., et al. (2001). Use of chemotherapy plus a monoclonal antibody against HER2 for metastatic breast cancer that overexpresses HER2. N. Engl. J. Med. *344*, 783–792.

Smith, J. (2005). Erlotinib: small-molecule targeted therapy in the treatment of non-small-cell lung cancer. Clin. Ther. *27*, 1513–1534.

Tzahar, E., Waterman, H., Chen, X., Levkowitz, G., Karunagaran, D., Lavi, S., Ratzkin, B.J., and Yarden, Y. (1996). A hierarchical network of interreceptor interactions determines signal transduction by Neu differentiation factor/neuregulin and epidermal growth factor. Mol. Cell. Biol. *16*, 5276–5287.

Weinstein, I.B., Begemann, M., Zhou, P., Han, E.K., Sgambato, A., Doki, Y., Arber, N., Ciaparrone, M., and Yamamoto, H. (1997). Disorders in cell circuitry

associated with multistage carcinogenesis: exploitable targets for cancer prevention and therapy. Clin. Cancer Res. *3*, 2696–2702.

Yonesaka, K., Zejnullahu, K., Lindeman, N., Homes, A.J., Jackman, D.M., Zhao, F., Rogers, A.M., Johnson, B.E., and Jänne, P.A. (2008). Autocrine production of amphiregulin predicts sensitivity to both gefitinib and cetuximab in EGFR wild-type cancers. Clin. Cancer Res. *14*, 6963–6973.

Yotsumoto, F., Sanui, A., Fukami, T., Shirota, K., Horiuchi, S., Tsujioka, H., Yoshizato, T., Kuroki, M., and Miyamoto, S. (2009). Efficacy of ligand-based targeting for the EGF system in cancer. Anticancer Res. *29*, 4879–4885.

Zhang, K., Sun, J., Liu, N., Wen, D., Chang, D., Thomason, A., and Yoshinaga, S.K. (1996). Transformation of NIH 3T3 cells by HER3 or HER4 receptors requires the presence of HER1 or HER2. J. Biol. Chem. *271*, 3884–3890.